

Shapes and dynamics of miscible liquid/liquid interfaces in horizontal capillary tubes

M. S. P. Stevar, A. Vorobev*

*Energy Technology Research Group, Faculty of Engineering and the Environment,
University of Southampton, SO17 1BJ, UK*

Abstract

We report optical observations of the dissolution behaviour of glycerol/water, soybean oil/hexane, and isobutyric acid (IBA)/water binary mixtures within horizontal capillary tubes. Tubes with diameters as small as 0.2 mm were initially filled with one component of the binary mixture (solute) and then immersed into a solvent-filled thermostatic bath. Both ends of the tubes were open, and no pressure difference was applied between the ends. In the case of glycerol/water and soybean oil/hexane mixtures, we managed to isolate the dissolution (the interfacial mass transfer) from the hydrodynamic motion. Two phase boundaries moving from the ends into the middle section of the tube with the speeds $v \sim D^{1/3}t^{-2/3}d^2$ (D , t and d are the coefficient of diffusion, time and the diameter of the tube, respectively) were observed. The boundaries slowly smeared but their smearing occurred considerably slower than their motion. The motion of the phase boundaries cannot be explained by the dependency of the diffusion coefficient on concentration, and should be explained by the effect of barodiffusion. The shapes of the solute/solvent boundaries are defined by the balance between gravity and surface tension effects. The contact line moved together with the bulk interface: no visible solute remained on the walls after the interface passage. Changes in temperature and in the ratio between gravity and capillary forces altered the apparent contact angles. The IBA/water system had different behaviour. Below the critical (consolute) point, no dissolution was observed: IBA and water behaved like two immiscible liquids, with the IBA phase being displaced from

*Corresponding author

Email address: A.Vorobev@soton.ac.uk (A. Vorobev)

the tube by capillary pressure (the spontaneous imbibition process). Above the critical point, two IBA/water interfaces could be identified, however the interfaces did not penetrate much into the tube.

Keywords: liquid/liquid interface, dissolution rate, binary mixture, non-Fickian diffusion, barodiffusion, dynamic surface tension, spontaneous imbibition, capillary tube

1. Introduction

Numerous engineering processes, such as vegetable oil extraction [1], enhanced oil recovery [2, 3], aquifer and soil remediation [4, 5], etc. [6, 7] are variations of the solvent-based (or miscible) displacement of a solute from a porous medium. Even an intravenous drug delivery could be considered as the dissolution of a liquid miscible droplet through porous body tissues [8]. The pore sizes are typically small, which makes the hydrodynamic flows within porous media being rather slow and as a result the diffusion and capillary effects play essential roles in the overall mass transport. The porous medium can be roughly represented as a network of interconnected capillary tubes [9, 10]. Using this so-called network approach, we define the aim of the current work as to understand the dissolution dynamics of binary mixtures within a single capillary tube, which is a necessary step to understand the miscible flows through a more complex porous matrix. We aimed to investigate the dissolution in tubes of very small diameters, when it is expected to be a diffusion-driven process. We managed to visualize the dissolution in capillary tubes with diameters as small as 0.2 mm , which are already comparable with the typical pore sizes in geological applications frequently assumed to be 0.1 mm and smaller. The pores however could be larger in the case of vegetable oil extraction.

In this work, the capillary tubes saturated with the solute phase are immersed into a solvent-filled thermostatic bath. When the pure components of a binary mixture are brought into contact we obtain a non-equilibrium binary system. Equilibration of the mixture to a thermodynamically stable state involves diffusive and hydrodynamic processes, and usually occurs very slowly (visible phase separation exists for hours after the initial contact of two completely miscible liquids). An example would be the dissolution of a honey droplet in water: honey is miscible in water in all proportions, but the droplet of honey remains visible in water for a rather long time period;

the honey droplet even retains its original shape while being agitated. It was concluded that the concept of interface needs to be employed to describe the dissolution in such a miscible system, and the interface should be endowed with dynamically variable surface tension. On molecular scale, the surface tension is explained by the differences in intermolecular forces existent in neighboring phases, which is applicable for both immiscible and miscible liquid mixtures, and which e.g. distinguishes miscible liquid from gaseous systems as in the latter case the intermolecular forces are negligible so no surface tension may appear. This idea was raised by Korteweg [11], Zeldovich [12] and others (see the book of Joseph and Renardy [13] for further details). Later the surface tension between miscible liquids was measured for different binary mixtures [14, 15, 16, 17]. Pojman et al. [18] even set up an experiment with honey/water system onboard of the International Space Station.

The dissolution, i.e. the mass exchange between the components of binary mixtures, is traditionally modelled as a process of inter-diffusion. A heterogeneous binary mixture is in equilibrium if the components have equal chemical potentials, when the interfacial mass transfer is absent despite the strong difference in concentrations. The rate of dissolution in a non-equilibrium system is determined by the difference in the chemical potentials between the neighboring phases (in the absence of temperature gradients). Since the chemical potential of an isothermal system is in general a function of concentration and pressure, then, in addition to the Fickian diffusion determined by concentration gradients, the mass transport can also be driven by pressure gradients [19]. Variations in pressure field can be induced by gravity and capillary forces. In mixtures of liquids with different densities, molecules of a heavier liquid tend to diffuse downwards. This gravity-driven diffusion transport is commonly referred as barodiffusion, and its intensity is proportional to the diffusion coefficient, the density contrast between the mixture components, and the gravity acceleration [20, 21, 22, 23, 24, 25]. The capillarity, that ultimately stems from the difference in intermolecular interactions within phases, gives rise to a potential barrier that molecules need to overcome in order to diffuse from one phase to another. The surface tension of an immiscible interface is so high that no molecules can cross the interface, while the surface tension of a miscible interface is considerably lower so some molecules are able to cross it. It is then obvious that diffusion of a molecule in the bulk and near the interface should occur differently, and hence the surface tension has a two-fold influence, affecting both the interface shape and the interfacial diffusion [23, 25].

Despite a seeming simplicity of the dissolution it is difficult to provide a simple estimate for the typical dissolution time. The knowledge of diffusion coefficient is not helpful, even if the simple Fickian diffusion law is accepted, which is frequently done in the case of completely miscible binary mixtures like glycerol and water [26]. A standard estimate for the diffusion time, L^2/D (with D being the coefficient of diffusion) is useless, since it is not clear what should be used as the typical size L in this formula. We are unaware of any experimental work in which the diffusion-driven dissolution of a liquid solute from a capillary tube has been studied. We may only name a theoretical work [27] in which the expression for the dissolution rate of a poorly dissolving liquid droplet placed in a capillary tube has been derived,

$$\frac{dL}{dt} = -\frac{C_1}{\sqrt{3-2C_1}}\sqrt{\frac{D}{t}} \approx -\frac{C_1}{\sqrt{3}}\sqrt{\frac{D}{t}}. \quad (1)$$

Here L is the length of the droplet, and C_1 is the solubility, i.e. the equilibrium solute concentration in the solvent. The mathematical model of [27] was reduced to Fickian diffusion process, and hence, the predicted dissolution rate follows the classical diffusion $t^{-1/2}$ time dependence.

In liquid mixtures the mass exchange between solvent and solute can be assisted by convective flows generated near the solute/solvent interface due to the dependence of the surface tension coefficient on concentration (the Marangoni convection) and by convective flows generated in the bulk phases due to gravity and due to the dependence of the mixture density on concentration (the solutal convection). The role of the solutal convection, for instance, could be estimated by the following analogue of the Rayleigh number,

$$Ra_s = \frac{g\Delta\rho L^3}{\eta D}, \quad (2)$$

where $\Delta\rho$ is the density contrast between the liquids, η is the mixture viscosity, and g is the gravity acceleration. Ra_s is constructed similar to the classical Rayleigh number and should be considered as the ratio between the diffusive and convective time scales. Again the typical size L is not well defined in formula (2), but it is generally presumed that the hydrodynamic flows are suppressed or at least significantly dampened in capillary tubes due to their small diameters.

In some sense, the effect of solutal convection can be also interpreted as the gravity current, also called the lock-exchange flow [28, 29, 30]. Such a

flow is induced if two liquids of different densities are initially separated by a vertical barrier, which is then removed. For instance, Zukoski [28] examined the motion of an air bubble in long closed tubes of different diameters ($> 0.5 \text{ cm}$) and with different inclinations. It was found that the bubble moves with a time-independent velocity

$$U = k \left(\frac{\Delta\rho}{\rho} g d \right)^{1/2}. \quad (3)$$

In (3), the coefficient k depends on the angle of inclination, viscous effects, and on the ratio between the gravity and capillary forces. In tubes of small enough diameter, when the effect of surface tension increases, the bubble motion ceased. The interplay between the gravity and capillary forces can be defined by the Bond number,

$$Bo = \frac{\Delta\rho g d^2}{\sigma}, \quad (4)$$

In [28], the bubble motion ceased completely for $Bo < 1.5$.

The motion of the liquid/liquid interface can be also induced by capillary forces. It is known that a less wetting liquid droplet could be displaced from the tube by the action of capillary forces (the so-called spontaneous imbibition process). The capillary forces are determined by the capillary pressure defined for the tubes of circular cross-section as

$$p_c = \frac{4\sigma \cos\theta}{d}, \quad (5)$$

where σ is the surface tension coefficient and θ is the contact angle. Formula (5) is written assuming that the meniscus is axisymmetric, and this symmetry may be broken by the gravity effect, i.e. when $Bo < 1$.

The speed of the interface driven by the capillary pressure is defined by the simple formula of Washburn [31],

$$v_{imb} = \frac{p_c}{32} \frac{d^2}{\eta L_0}. \quad (6)$$

Here L_0 is the length of the tube. In the open capillary tube there are two solute/solvent interfaces, and the capillary forces should have no cumulative effect on the droplet motion. It should be also taken into account that the

miscible system is not in its thermodynamic equilibrium, which means that both the surface tension coefficient and the values of the contact angle in formula (5) are time-dependent. The ratio between the diffusion rate and speed v_{imb} determines whether this time-dependence is important.

The spontaneous imbibition in capillary tubes has been experimentally studied by Washburn [31] and Chertcoff et al. [32]. They found that formula (6) correctly predicts the propagation of a more wetting liquid into the capillary tube.

In other related studies, Taylor [33] and Cox [34, 35] examined the displacement of a liquid by air from the capillary tube driven by external pressure difference. Similar experiments were also fulfilled by Soares et al. [36] with the use of two immiscible liquids. They noted that air (or an injected liquid in the case of Soares et al.) breaks through the center part of the tube's cross-section, and some amount of the liquid, that initially occupied the tube, remains on the tube's walls. This research was later extended to address the displacement of miscible liquids [37, 38, 39]. The experiments with miscible interfaces were carried out with mixtures of glycerol and water and of two different silicon oils. The tube was initially saturated with a more viscous liquid, which was then displaced by a less viscous liquid by applying an external pressure gradient. The velocity of the induced hydrodynamic flow substantially exceeded the diffusion rate with the typical Peclet numbers of about 10^4 . The liquid/liquid dissolution was not considered in these works.

The interface smearing rates were measured by Viner and Pojman [24], who examined the evolution of the IBA/water mixture in a vertical cuvette heated to supercritical temperatures by using the laser line deflection technique. They noticed that the homogenization of IBA/water mixture (the components were taken in equal volumes of 0.6 ml each) lasts for about 25 hours at the temperature of $30^{\circ}C$, and reported that the transition zones that separate the water and IBA phases (the interphase boundaries) slowly grew into the IBA volume with $t^{0.06}$ time dependence. Similar experiments were undertaken by Petitjeans and Maxworthy [37] in order to measure the diffusion coefficient at the glycerol/water interface. They found that the transition zone slowly grew into the glycerol phase and fully disappeared after at least 6 hours under room temperature. Dambrine et al. [40] studied the interdiffusion of pure water and 40% glycerol/water mixture within a microchannel using Raman imaging and found that the interface thickness grows as $(Dt)^{1/2}$, but they also noted shifting of the phase boundary into

Table 1: Density and viscosity coefficients for pure glycerol, soybean oil, IBA, water and n-hexane at $20^{\circ}C$. [13, 43, 44]

Substance	$\rho, g \times cm^{-3}$	$\eta, Pa \times s$
Glycerol	1.26	1.41
Soybean oil	0.917	0.069
IBA	0.95	$1.1 \cdot 10^{-3}$
Water	1.00	$1.01 \cdot 10^{-3}$
n-Hexane	0.659	$0.326 \cdot 10^{-3}$

glycerol phase.

2. Materials and Methods

2.1. Binary mixtures

In our work, we examine the evolutions of glycerol/water, soybean oil/hexane and IBA/water binary mixtures. All chemicals having high purities were purchased from Fisher Scientific or Sigma Aldrich and were used as received.

Glycerol and water and soybean oil and hexane are miscible in any proportions under all temperatures. The IBA/water mixture is characterized by the upper critical solution temperature, $T = 26.2^{\circ}C$ [41, 42, 15]. At temperatures above the critical point, the mixture components are miscible in any proportions. Below the critical point, only small amounts of IBA are completely miscible in water, and if a larger droplet of IBA is added, then IBA and water phases will inter-diffuse until the equilibrium concentrations, C_1 and C_2 , are established. The values of C_1 and C_2 are temperature dependent and can be obtained from the phase diagram available e.g. in the paper of Pojman et al. [15].

The values of density and viscosity coefficient for the pure substances are summarized in table 1. The mixture densities are concentration-dependent, but it is known that a ‘simple mixture’ approximation,

$$\frac{1}{\rho} = \frac{1 - C}{\rho_1} + \frac{C}{\rho_2}, \quad (7)$$

works well. For instance, this approximation has an 1% accuracy for the glycerol/water mixture [13], which has been also confirmed by our measurements. In equation (7), ρ is the mixture density, while ρ_1 and ρ_2 are the densities of the pure substances, and C is the concentration defined as the

mass fraction of solute. The mixture viscosity also depends on concentration. For the glycerol/water mixture measurements of the viscosity as a function of concentration can be found in the works of Segur and Obestar [43] and Kim and Ju [45]. The values of viscosity of the IBA/water mixture in supercritical conditions are available in the work of Ouerfelli et al. [44].

The values of diffusion coefficient for the glycerol/water mixture under different temperatures and for different compositions can be found in the works of Petitjeans and Maxworthy [37], Rashidnia and Balasubramaniam[46], and D’Errico et. al[47]. For reference, the mutual diffusion coefficient at room temperature equals $1.6 \times 10^{-10} m^2 s^{-1}$ at an interface between pure glycerol and water, the magnitude of diffusion coefficient linearly drops for interfaces between glycerol/water mixture and pure water and gets ten times smaller in pure glycerol [37, 47]. The IBA/water mutual diffusion coefficient is zero in the critical point and above the critical point the diffusion coefficient grows as $D = D_0 \left(\frac{T-T_c}{T_c} \right)^\nu$, where $\nu = 0.664$ and $D_0 = 5.9 \times 10^{-10} m^2 s^{-1}$ [41, 48, 49, 50, 51]. The diffusion coefficient equals $1.3 \times 10^{-11} m^2 s^{-1}$ at $27^{\circ}C$ and $2.8 \times 10^{-11} m^2 s^{-1}$ at $30^{\circ}C$. We could not find in the literature values of the IBA/water diffusion coefficient for temperatures below the critical point.

The surface tension coefficient is traditionally defined only for the equilibrium states of a binary mixture. Glycerol and water form a homogeneous solution in equilibrium, and no surface tension coefficient is traditionally associated with miscible interfaces. The dissolution is however a very slow process and the phase separation could be observed for long time periods, so the effective surface tension could be introduced. The estimations of Petitjeans and Maxworthy [37] show that the surface tension coefficient to be associated with the glycerol/water interface is approximately $0.4-0.5 dyn \times cm^{-1}$. In the case of IBA/water mixture, the equilibrium heterogeneous states can exist at temperature lower than the critical point. The IBA/water surface tension coefficient depends on temperature, decreasing as the mixture temperature approaches the critical point. For instance, the surface tension coefficient equals $0.06 dyn \times cm^{-1}$ at $T = 24^{\circ}C$ [49, 52]. The equilibrium surface tension is zero at and above the critical temperature. Since thermodynamic equilibration occurs slowly the dynamic surface tension could be introduced. These dynamic values were measured by Pojman et al. [15] using the spinning droplet tensiometry technique. Values of the order of $0.01 dyn \times cm^{-1}$ were reported for temperatures slightly above the critical point.

We could not find in the literature the above-mentioned material coef-

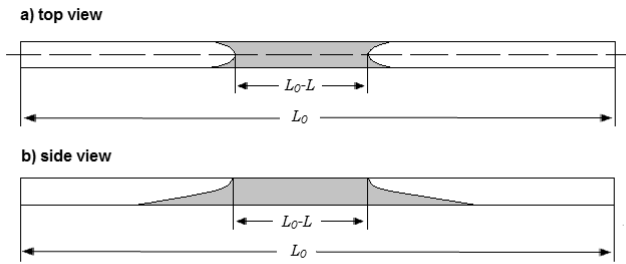


Figure 1: A schematic view of the solute/solvent mixture saturating the capillary tube.

ficients for the soybean oil/hexane mixture. Only in the paper of Wu and Lee [53] the theoretical estimations of the mutual diffusion coefficient for the mixture of soybean oil and hexane are given, being $9.1 \times 10^{-10} m^2 s^{-1}$ at $25^{\circ}C$.

2.2. Experimental rig

In the experiments the tubes were filled with solute (glycerol, soybean oil or IBA) and then immersed into a thermostatic transparent solvent-filled (water or hexane) bath of dimensions $100 \times 20 \times 20 cm$. The tubes were placed horizontally with both ends being open. No pressure gradient was applied between the ends of the tubes. The capillary tubes had circular and square cross-sections, different inner ($0.2 - 1.6 mm$) and outer diameters ($0.33 - 7 mm$), various lengths ($2 - 50 cm$) and were made of fused quartz or borosilicate glass. The tubes were purchased from Vitrocom Inc and Fisher Scientific.

The experiments were performed at various temperatures in the range of $20^{\circ}C - 50^{\circ}C$. The temperature in the water bath was controlled with a Grant digital thermostat (GD100, stability at $37^{\circ}C$ is $0.05^{\circ}C$); the homogeneity of the solvent temperature was checked in several reference points with a Checktemp1 thermometer by Hanna Instruments (accuracy is $0.3^{\circ}C$). Solute and solvent temperatures become equal at the time the tube is immersed into the bath. Simple estimations show that the thermal equilibration takes less than 1 minute even for the thickest tubes used, i.e. almost instantly in comparison with the duration of the experiments.

The shape and the position of solute/solvent interfaces were recorded with a system including a CCD camera (LaVision Imager 3S) with Questar lenses (QM100 Model #30003, with working distances in the range $15 - 35 cm$, and magnification up to 34 times at the image plane), a diffuser (LaVision, VZ illumination high-efficiency diffuser) and a diode laser (Oxfordlaser Firefly

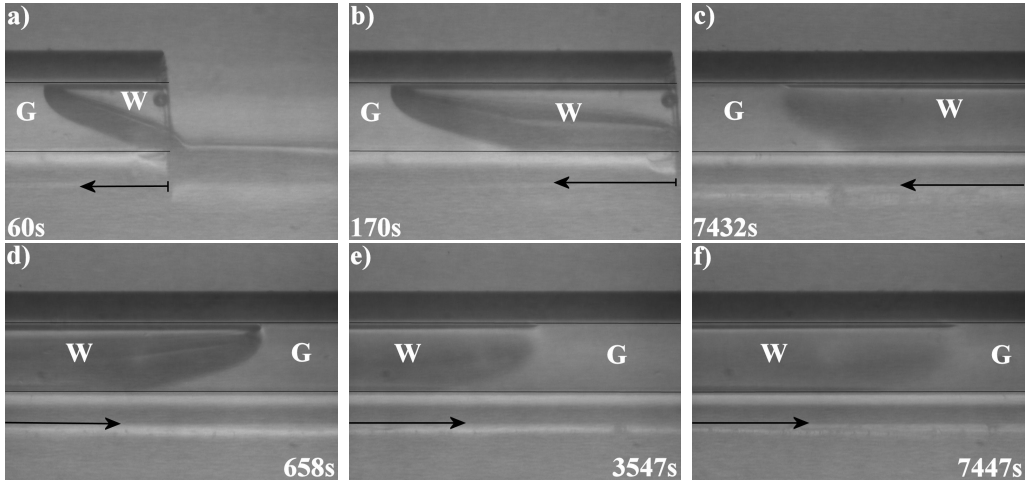


Figure 2: The shapes of glycerol/water interphase boundaries within a capillary tube with square cross-section at different time moments. (a-c) and (d-f) sequences show the two interfaces propagating from opposite ends of the tube. The tube has diameter $d = 0.4\text{ mm}$ and length $L = 10\text{ cm}$, the mixture temperature is $T = 20^{\circ}\text{C}$. The exact time moments are shown in the pictures. 'W' and 'G' letters indicate the water and glycerol phases. The arrows indicate the directions of the interface motion.

system) used for illumination. To improve the image contrast the solute-liquids were coloured with methylene blue, Sudan IV, or eriochrome black T dyes purchased from Sigma Aldrich. In some experiments solid microparticles were dispersed in the solute phase to detect any hydrodynamic flows in the tube.

The whole tube is schematically depicted in figure 1. The snapshots shown below show different sections of the tube.

3. Results and discussion

3.1. Glycerol-water mixture

Glycerol and water are miscible in any proportions. One would expect that a glycerol/water interphase boundary would slowly smear in time due to inter-diffusion, while the boundary itself should remain stationary in the absence of hydrodynamic flows. In the experiment we observe that water penetrates into the tube forming two clear glycerol/water interfaces at the ends. The interface smearing occurs at considerably lower rates than the interface propagation speeds. Generally, the interfaces remain visible for

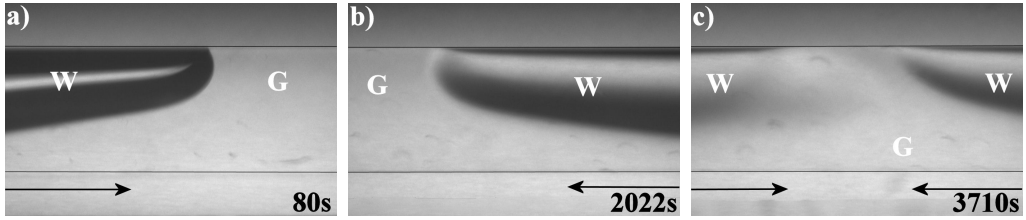


Figure 3: The time progression of the glycerol/water interface into a capillary tube of circular cross-section. The diameter of the tube is $d = 0.6\text{ mm}$ and the length is $L = 5\text{ cm}$. The temperature is maintained at $T = 30^\circ\text{C}$. Only the tips of the interfaces are shown, but the contact lines are closed within the tube. All notations as in figure 2.

time periods up to 10^4s . Their time evolution is shown in figures 2 and 3. In shorter tubes, the experiment could be carried out until the two opposite interfaces meet (see figure 3c). The interfaces of the shown shape remain stable for quite long time periods and experience shape changes only when they become too diffusive or at their point of fusion.

Figure 2a shows the initial evolution of the glycerol/water boundary. This stage lasts for about 1 minute. Diffusion is negligible at this stage, and glycerol, being heavier than water, is displaced from the tube due to gravity. The interfacial boundary never breaks up in the sense that no new glycerol or water droplets are formed. When the contact line is closed up within the tube the interface shape stabilizes (gravity and capillary forces are balanced).

For the glycerol/water binary mixture the Bond number defined by equation (4) is less than 0.1, which indicates the dominance of capillary over gravity forces. Nevertheless, figures 2 and 3 show menisci are affected by gravity, which could signify that the glycerol/water surface tension coefficient of Petitjeans and Maxworthy [37] is an over-estimation. The gravity forces become less important for menisci in the tubes of smaller diameters, which could be noted by comparison of figures 2 ($d = 0.4\text{ mm}$) and 3 ($d = 0.6\text{ mm}$). The interface becomes less inclined in tubes of smaller diameters, but the gravity effects remain important even in the tubes of 0.2 mm diameter. We found no dependence of the interface shape on temperature at least for the investigated range of $20^\circ\text{C} - 50^\circ\text{C}$. Another surprising conclusion that can be drawn from figure 2 is that the more diffusive the phase boundary becomes the less inclined it is indicating that the ratio of capillary over gravity forces even increases for the diffusive interfaces.

In figures 2 and 3 one sees that glycerol is a more wettable liquid than

water. The apparent contact angles at the upper and lower parts of the interface are different. The shape of the contact line does not change while the interface moves into the tube indicating that no visible glycerol phase remains on the tube walls after the passage of the interface.

The rate of the glycerol dissolution should be defined as the rate of glycerol removal from the tube. The water phase in the tube obviously contains some dissolved glycerol, an amount which we cannot measure. For this reason, the dissolution rate was defined as the propagation speed of the glycerol/water phase boundary. We measured the length of the tube occupied by the water phase L , calculated as $L = L_0 + x_1 - x_2$, where L_0 is the tube's length and x_1 and x_2 are the coordinates of the first and second interfaces (the reference point for the x -coordinate is at one of the tube's ends). Initially the tube is filled with the solute, and L is zero, later water diffuses into the tube, and L grows (see figure 1). These measurements were obtained without the use of the optical rig and are shown in figure 4. We found that the rate of water propagation is independent on the length of the tube, and each curve in figure 4 aggregates the data from several experiments carried out with tubes of different lengths. One can see that the interfaces propagate faster in the tubes of larger diameters and the dissolution rates grow with the increase of temperature.

The interface propagation slows down upon its penetration into the tube. The plots of figure 4 are re-plotted in logarithmic scales in figure 5. The new figures show that the time evolution of L can be approximately represented by two power laws, $t^{2/3}$ in the beginning and $t^{1/3}$ starting from some point. The time moments when the dependence is changed depend on the tube diameter and temperature, but their values of about 100 s indicate that the $t^{2/3}$ -dependence corresponds to the initial gravity-driven displacement of the glycerol phase (figure 2a), while the later $t^{1/3}$ dependence should characterize the motion of the stabilized interfaces. In the larger tubes, $t^{2/3}$ -dependence is observed for longer time periods, while the dissolution rate in smaller tubes is solely defined by the $t^{1/3}$ power law.

The data of figure 4 could be used to obtain the interface speeds derived as $v = \frac{1}{2} \frac{dL}{dt}$. In addition to the data of figure 4, the speeds of the interface propagation within the smaller tubes were obtained from the analysis of the image sequences. The interface speeds could be approximated by $t^{-1/3}$ at initial moments and by $t^{-2/3}$ at later stages. In the smallest tubes, with diameters of $d = 0.2mm$ and $d = 0.4mm$, only one time-dependence, $t^{-2/3}$, could be identified, which is shown in figure 6b.

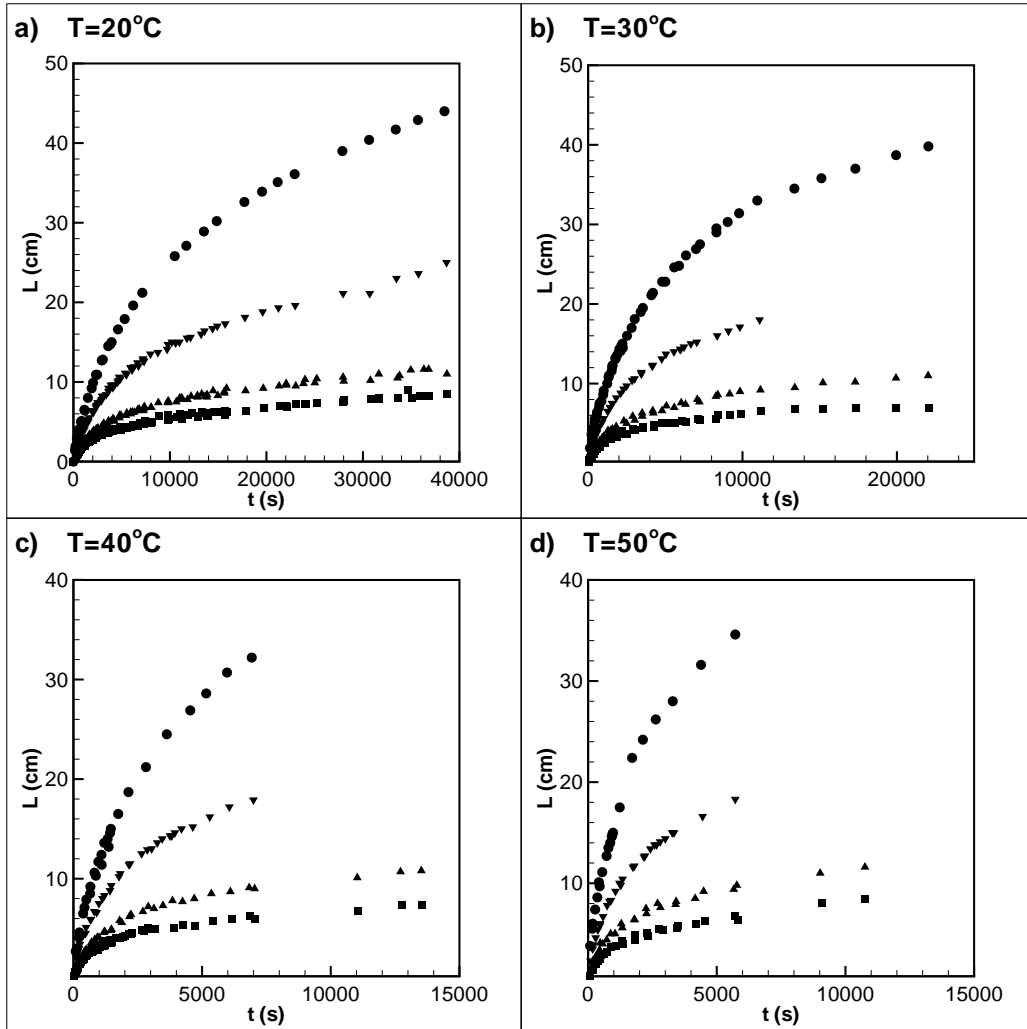


Figure 4: The length of the tube occupied by the water phase as a function of time. Tubes with circular cross-sections and diameters of 0.6 mm (■), 0.8 mm (▲), 1.2 mm (▼) and 1.6 mm (●) were used. The experiments were conducted under different temperatures: a) $T = 20^{\circ}\text{C}$, b) $T = 30^{\circ}\text{C}$, c) $T = 40^{\circ}\text{C}$ and d) $T = 50^{\circ}\text{C}$.

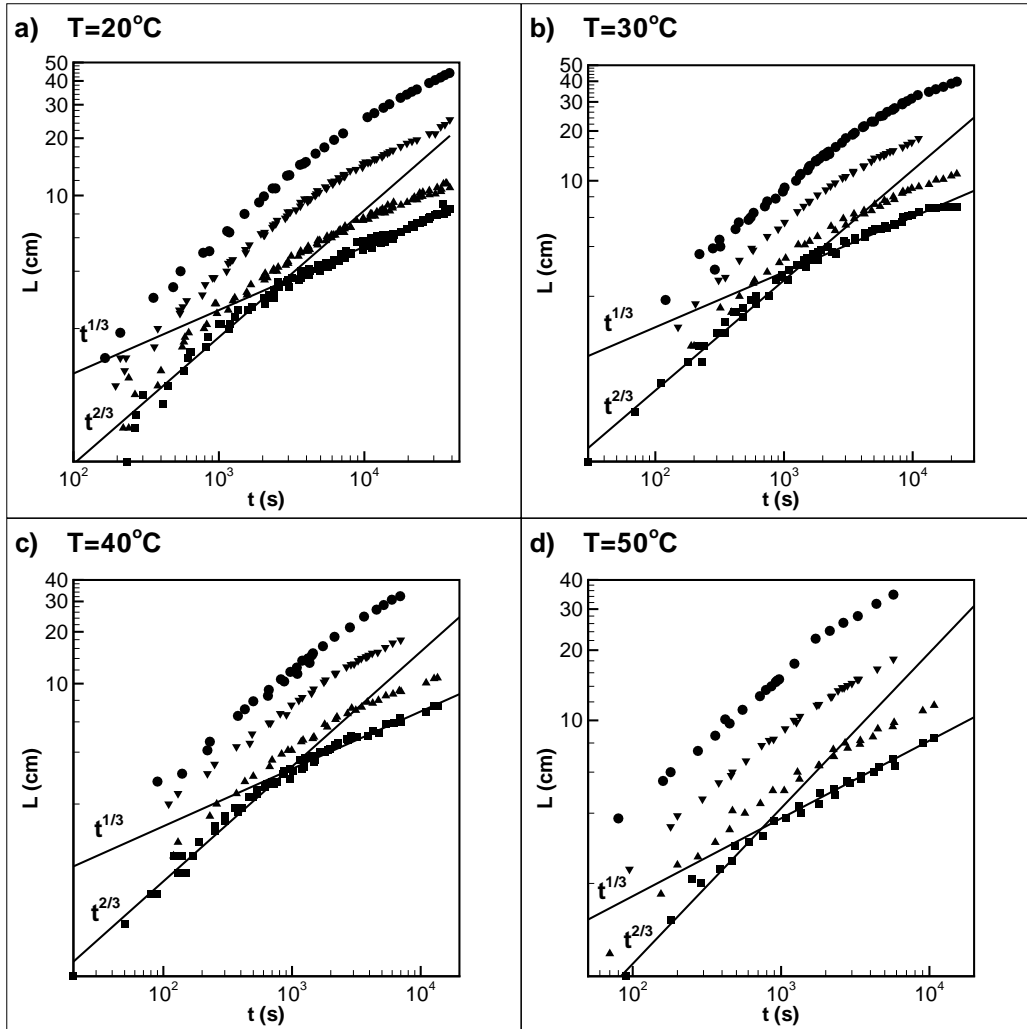


Figure 5: The length of the tube occupied by the water phase as a function of time in logarithmic scales. Tubes with circular cross-sections and diameters of 0.6 mm (\blacksquare), 0.8 mm (\blacktriangle), 1.2 mm (\blacktriangledown) and 1.6 mm (\bullet) were used. The experiments were conducted under different temperatures: a) $T = 20^\circ\text{C}$, b) $T = 30^\circ\text{C}$, c) $T = 40^\circ\text{C}$ and d) $T = 50^\circ\text{C}$.

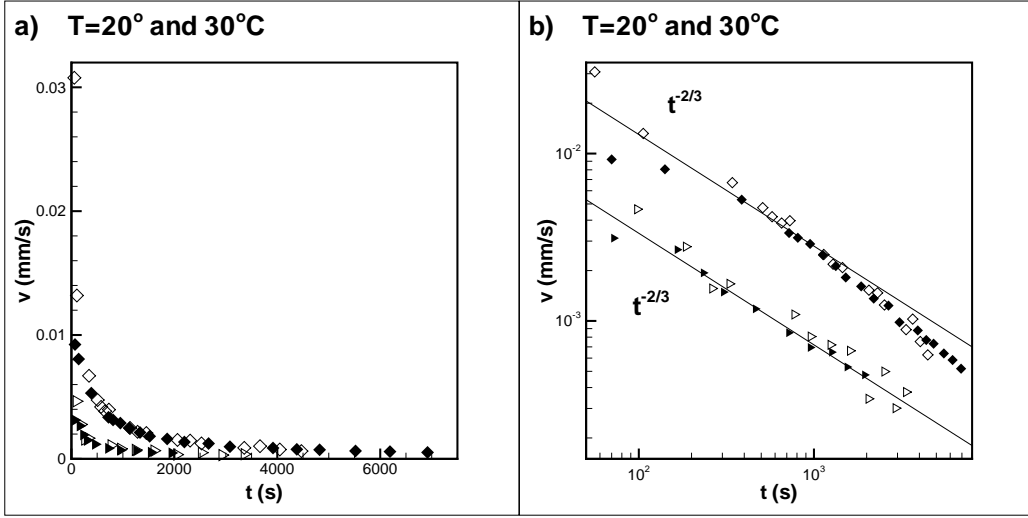


Figure 6: The speed of the interface propagation as a function of time in capillary tubes of square cross-section with diameters $d = 0.2\text{mm}$ (\blacktriangleright) and $d = 0.4\text{mm}$ (\blacklozenge) at temperatures of $T = 20^\circ\text{C}$ (filled symbols) and $T = 30^\circ\text{C}$ (empty symbols). (a) The data are shown in normal coordinates. (b) The same data are plotted in logarithmic coordinates.

The physical mechanisms that define the glycerol removal from the tube need to be clarified. There are two interfaces formed moving towards each other; obviously, their propagations cannot be explained by spontaneous imbibition. Estimates of the Bond number are less than 0.1, and the solute phase is locked by the interfaces. Hence, the gravity currents should not drive the motion either. No pressure difference between the tubes ends was imposed, consequently, no externally generated hydrodynamic flow should develop. The internally generated convective flows may be induced due to density contrast (the solutal convection) and due to the dependence of the surface tension on concentration (the Marangoni convection). For instance, the intensity of solutal convection is characterized by the Rayleigh number (2), that can be estimated as $Ra_s \sim 0.1$ for the glycerol phase and $Ra_s \sim 10^2$ for the water-rich phase by using the smallest tube diameter (0.2mm) as the typical size. That means the solutal convection may exist in the water-rich phase.

The initial gravity-driven penetration of the water phase could also be interpreted as the solutal convection (or as the gravity current). To experimentally assess the role of hydrodynamic flows at later time moments, we

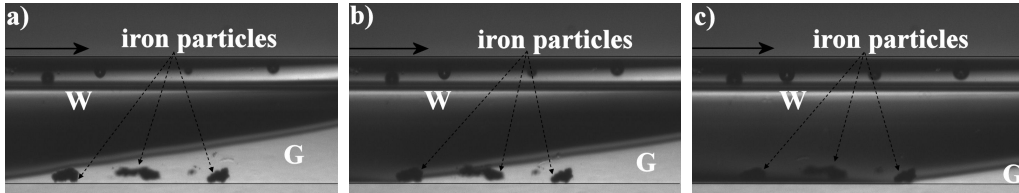


Figure 7: The evolution of the interface shape within a tube with $d = 0.6\text{mm}$. The temperature is $T = 25^{\circ}\text{C}$. The glycerol phase contains metallic (iron) particles. The time interval between the shown snapshots (a) and (b) is 120s ; the interval between (b) and (c) is 310s . Several small droplets appearing in the upper parts of the images are air bubbles in the water bath outside the tube.

set up the experiments with the use of small metallic (iron, 99%) particles with diameters $< 212\mu\text{m}$ dispersed in the glycerol phase. Since the studied processes are rather slow, all particles were settled on the bottom of the tube (see figure 7). We observed that while the interface is passing through the section of the tube with particles, the particles remain immovable. The interface shape remains almost unperturbed by the obstacles. No hydrodynamic flows were detected in these experiments.

Thus, the motion of the interfaces should be explained by the interfacial mass transport, which should be a diffusion-based process, but cannot be reduced to sole Fickian diffusion. Firstly, because the rate of the interface propagation does not follow the classical time dependence of the diffusion theory, $t^{1/2}$. Secondly, the use of the standard estimate for the diffusive time-scale gives an enormous value, $\tau_d = \frac{L^2}{D} \approx 10^8\text{s}$, if L is taken as the tube length. The phase boundaries move considerably faster.¹ Next, we analyzed how the interface speed depends on the tube's diameter and temperature. For this, we introduced the coefficients A and B defined by the expressions, $L = At^{2/3}$ and $L = Bt^{1/3}$. The dissolution rate is obviously proportional to

¹The diffusion coefficient of glycerol/water binary mixture strongly depends on concentration. The mutual diffusion coefficient in glycerol-rich phase is about ten-fold lower than in water-rich phase [37, 47]. Such a strong dependence allows the front-type penetration of a solvent into a solute-saturated tube to be mathematically reproduced on the basis of the Fickian law, but the resultant front's speed would be always proportional to $t^{1/2}$ if only Fickian transport is taken into account [54]. The front-type dissolution in polymer mixtures with the front's speeds different from $t^{1/2}$ is known, see e.g. [55]. In [55], such a behaviour is associated with viscoelastic properties of polymers, but such an explanation and a developed mathematical model is not acceptable for the glycerol/water mixture.

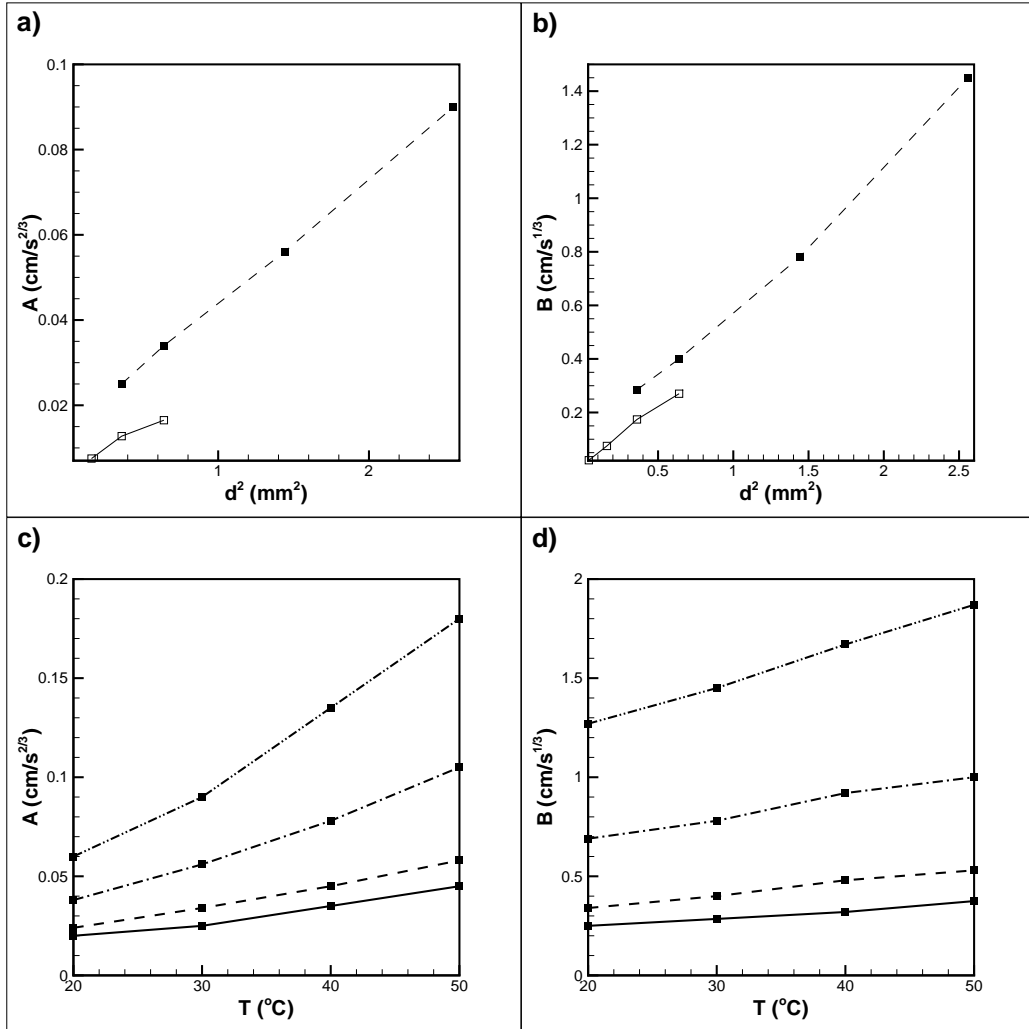


Figure 8: (a,b) Coefficients A and B versus the square diameter of the tube. The filled symbols correspond to the data derived from 4 (larger tubes); the empty symbols are for the data obtained from the set of optical measurements (smaller tubes). The data are obtained for the experiments conducted at the temperature $T = 30^\circ\text{C}$. (c,d) Coefficients A and B for different temperatures for the larger tubes: $d = 0.6\text{ mm}$ (solid line), $d = 0.8\text{ mm}$ (dash line), $d = 1.2\text{ mm}$ (dash-dot line), and $d = 1.6\text{ mm}$ (dash-dot-dot line).

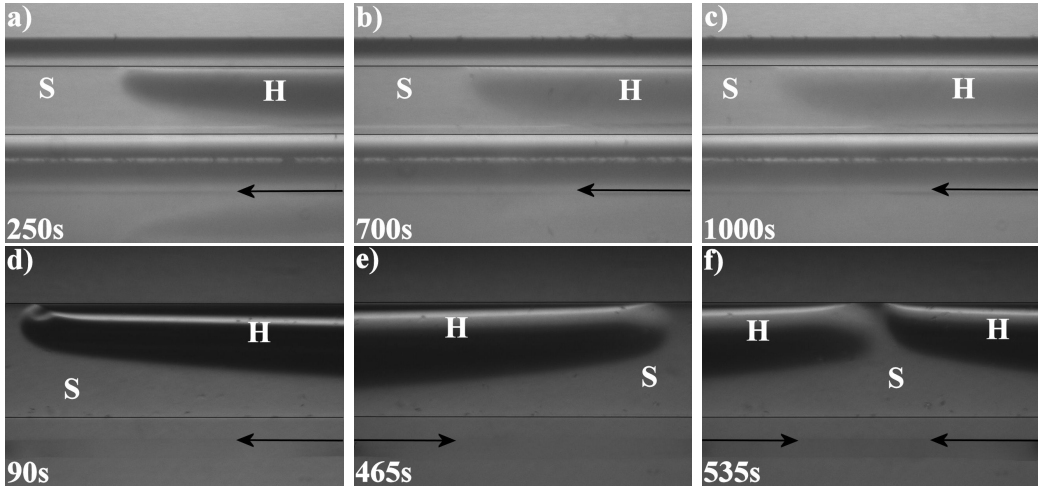


Figure 9: The soybean oil/hexane interphase boundaries at different time moments. The snapshots are obtained for the experiments conducted with a tube of square cross-section with diameter $d = 0.4 \text{ mm}$ and length $L = 10 \text{ cm}$ (a-c) and with a tube of circular cross-section with diameter $d = 0.6 \text{ mm}$ and length $L = 4 \text{ cm}$ (d-f). In (d-f) only tips are shown, but the contact lines are closed within the tube. Temperature is $T = 20^\circ\text{C}$. ‘H’ and ‘S’ letters indicate the soybean oil and hexane phases.

these coefficients. Figure 8 clearly shows that A and B grow with the increase of the tube’s diameter and temperature. We found that the dissolution rate is proportional to the square of the tube’s diameter. This is a surprising result, that also contradicts the assumption that the interface motion is driven by Fickian interdiffusion, for which the dissolution rate should be independent of the value of the tube’s diameter.

We conclude that the phase boundaries are driven by the barodiffusion effect. We saw that the solute/solvent interfaces are inclined, i.e. their shapes are affected by gravity. As the tube diameter decreases, the gravity influence weakens and the motion of the interface is slower. A strictly vertical interface is not affected by gravity, and hence does not move due to barodiffusion. The inclined interfaces seen in the experiments are driven by barodiffusion, while their smearing is defined by Fickian diffusion.

3.2. Soybean oil-hexane mixture

We also carried out experiments with the soybean oil/hexane binary mixture. Hexane and soybean oil are miscible in any proportion. Currently hexane is the most commonly used solvent for the vegetable oil extraction.

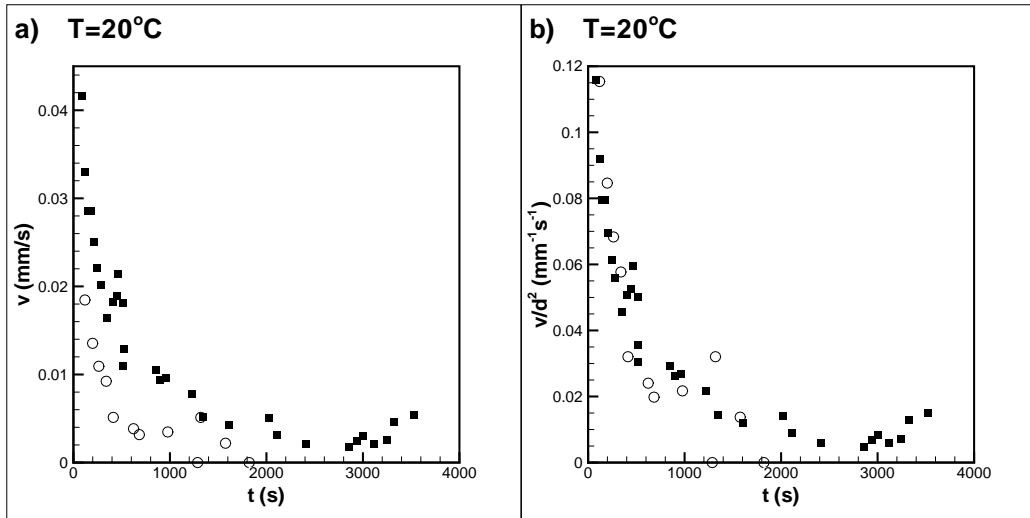


Figure 10: (a) The time evolution of the speed of propagation of soybean oil/hexane interfaces in tubes of different diameters. (b) The interface speed divided by the square diameter of the tube versus time. The data are collected from the experiments with the tubes of diameter $d = 0.4$ mm (\circ) and $d = 0.6$ mm (\blacksquare). The experiments are conducted under temperature $T = 20^\circ\text{C}$.

The dissolution of soybean oil from the tube occurred similar to the one of glycerol. The time progression of the soybean oil/hexane phase boundaries is shown in figure 9. Since the interface shape is determined by the balance between gravity and capillary forces, the surface tension coefficient for the soybean oil/hexane interface can be estimated from comparison of figures 9d and 3a. The soybean oil/hexane interface is inclined twice stronger than the glycerol/water interface in the same tube. Since the glycerol/water and soybean oil/hexane mixtures have similar density contrasts, we conclude that the surface tension coefficient for the soybean oil/hexane mixture should be of the same order, but lower. Roughly, the surface tension coefficient for the soybean oil/hexane interface is of the order of $0.1 \text{ dyn} \times \text{cm}^{-1}$.

Similar to the glycerol/water interfaces, the phase boundaries between soybean oil and hexane diffuse in time but at considerably slower rates than the speeds of the interfaces motion. The propagation speeds of the phase boundaries are shown in figure 10a. Again, we found that the speed of the interface propagation follows $t^{-1/3}$ and $t^{-2/3}$ power laws at the initial (convective) and later (diffusive) evolutions, and that the interface speed is proportional to the area of the tube's cross-section. The latter statement

is confirmed by figure 10b where the ratio of the interface speed over the square of the tube's diameter is plotted versus time; the curves for the tubes of different diameters are merged by this modification.

The diffusion coefficient for the soybean oil/hexane mixture is higher than for the glycerol/water interface (for similar solute concentrations), and both smearing and motion of the phase boundaries occur faster. This confirms that the observed dissolution of binary mixtures is a diffusion-based process. We also found that the propagation speeds of the soybean oil/hexane interface are about 1.7 times faster (e.g. for $d = 0.4\text{mm}$ and $T = 20^{\circ}\text{C}$) than the corresponding speeds of the glycerol/water phase boundaries. This indicates that the interface speed is proportional to the cubic root of the diffusion coefficient, $v \sim D^{1/3}$.

3.3. Isobutyric acid-water mixture

The experiments were also conducted with the use of the isobutyric acid (IBA)/water binary mixture. This binary mixture has a phase diagram with an upper critical solution temperature, $T_c = 26.2^{\circ}\text{C}$. In our experiments, IBA volumes contained in the tubes are negligibly small in comparison with the volume of the solvent, and all immersed IBA is finally dissolved even if the mixture temperature is below the critical (consolute) point.

We found that the components of the binary mixture are separated by a visible interfacial boundary; below the critical point the interface is always sharp; above the critical point the interfaces become quickly diffusive. The dissolution scenario is different in the experiments conducted at temperatures below and above the critical point. In under-critical conditions we always observe the propagation of only one phase boundary into the tube, the second interface remaining attached to the opposite end. In the experiments conducted under super-critical temperatures, both interfaces start moving into the tube at the initial moments. At some time moment one interface, being still quite close to the end of the tube, stops, while the second interface continues its motion further into the tube.

The shapes of the stabilized IBA/water interfaces strongly depend on the mixture temperature, as it can be seen in figure 11. Below the critical point the role of capillary forces is sufficiently strong to make the interface being vertical at least in the tubes of smaller diameters (see figure 11a,d). For these temperatures, the estimation of the Bond number (4) produces $Bo < 0.01$, indicating significant dominance of the capillary effects. The effect of gravity is non-visible, the meniscus having axisymmetric shape. In

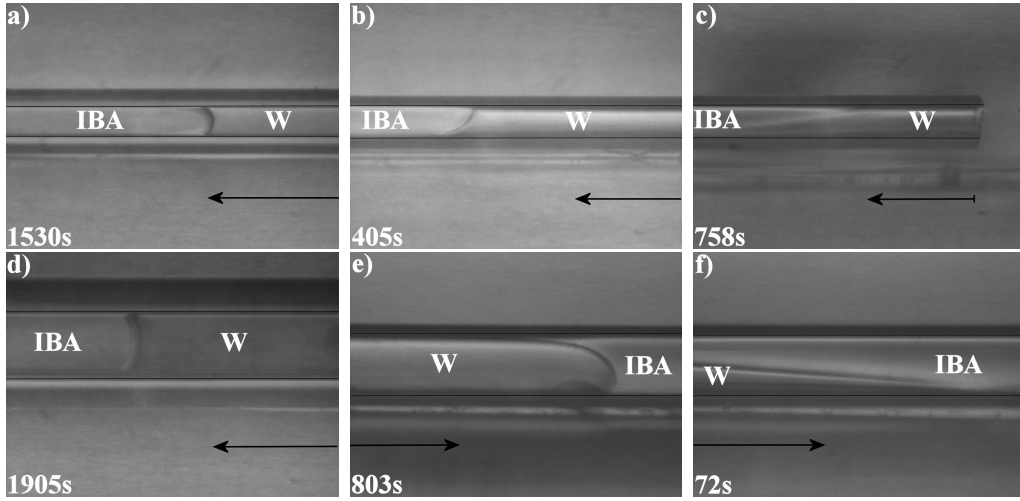


Figure 11: The shape of the IBA/water interface in capillary tubes of square (a,d) and circular (b,c,e,f) cross-sections with diameters of 0.2mm (a-c) and 0.4mm (d-f) and lengths of 10cm under different temperatures: a,d) $T = 20^\circ\text{C}$, b,e) $T = 26^\circ\text{C}$, and c,f) $T = 30^\circ\text{C}$. ‘IBA’ and ‘W’ designate the IBA and water phases, respectively.

the tubes with diameter of 0.6mm and larger, the apparent contact angles get slightly different at the upper and lower parts of the tube. The gravity effects become also apparent in the smaller tubes but at the near-critical temperatures when the surface tension decreases (figure 11b,e). At higher temperatures, higher than 30°C , the surface tension becomes negligible so the IBA phase is displaced due to gravity (figure 11c,f). The wetting properties of the IBA/water mixture seem to be also temperature dependent. In under critical conditions water looks to be more wettable than IBA. Closer to the critical temperature and above the visible contact angles have different signs at the lower and upper sides of the tube.

Let us now discuss how the IBA becomes removed from the tube. At temperatures below the critical point, we observed that the interface always propagates from one side of the tube only, being obviously driven by the capillary pressure, i.e. representing the process of spontaneous imbibition. As in the glycerol/water experiments, the contact line moves together with the main interface, so no IBA phase seems to be left on the walls of the tube after the interface passage.

At the time of the initial IBA/water contact, in the capillary tubes with larger diameters $d \geq 0.6\text{mm}$, the propagating interface experiences quite

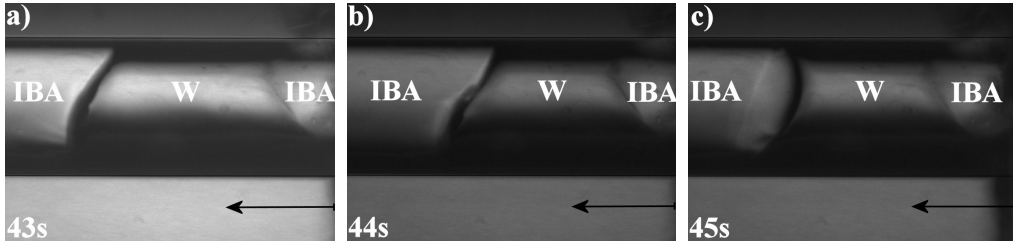


Figure 12: The initial evolution of the IBA/water interface in a capillary tube of circular cross-section with diameter of 0.8 mm and length 10.3 cm at temperature $T = 20^{\circ}\text{C}$.

complex modifications of its shape as shown in figure 12. The initially vertical IBA/water boundary is unstable and breaks down: the water phase under-rides IBA forming a new isolated droplet of IBA phase at the end of the tube; the new IBA/water interface propagates further in the tube. This initial evolution, during which two IBA/water interfaces could be noticed at one end, typically takes about $\sim 10\text{ min}$. Finally, the under-ridden IBA droplet is displaced/dissolved from the tube. The newly formed IBA/water interface is more stable and does not experience any further instabilities. The complex evolution at the time of entrance of the water phase into the tube was more evident at near-critical temperatures when the surface tension is lower. The interface never breaks in the capillary tubes with diameters $\leq 0.4\text{ mm}$ at temperatures lower than 25°C , when the interfaces were always stable from the start of the experiment.

In addition, we observed that the meniscus shape experiences oscillations as demonstrated in figure 13a-c. The amplitude of meniscus oscillations is larger in the tubes of larger diameters and also in experiments conducted under near-critical temperatures. The time-resolution of the used visual rig was sufficient to estimate the period of oscillations which was found to be of the order of 2 s in the tube of diameter 0.8 mm . We also found that the penetration of the solvent from one end of the tube was accompanied by the visible displacement of the solute from the opposite end (figure 13d-f), where the droplets of IBA are periodically displaced and detached from the end of the tube with the period equal to the period of the meniscus oscillations. The droplets are seemingly being detached when the buoyancy force overcomes the adhesion between the IBA droplet and the outer tube's wall, which defines the period of meniscus oscillations.

Another question is when the symmetry of the experiment is broken. Two

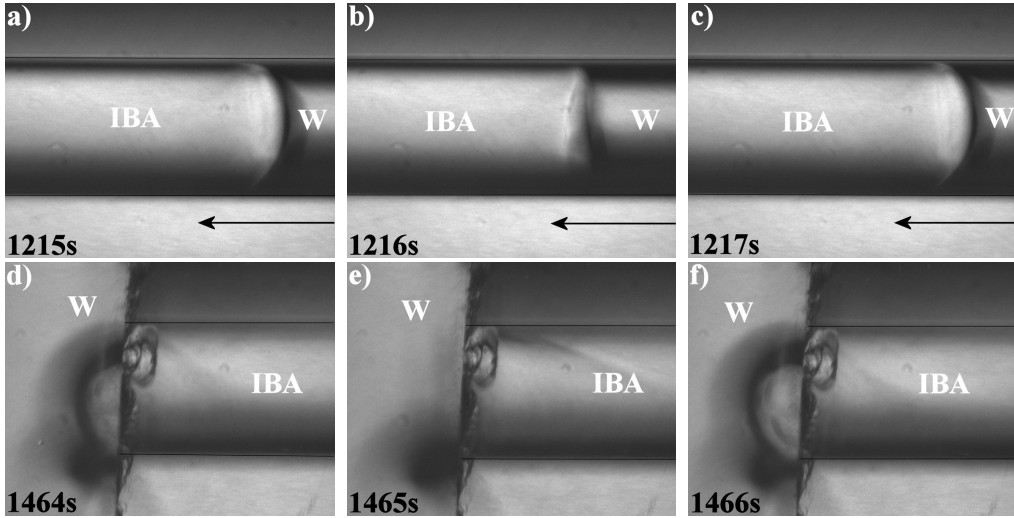


Figure 13: (a-c) Oscillations of the stabilized interface in a capillary tube of circular cross-section. (d-f) The formation and detachment of the IBA droplet at the opposite end of the tube. The tube has a diameter of 0.8 mm and length 10.3 cm . The temperature is maintained at $T = 20^{\circ}\text{C}$.

ends of the tube are equivalent, two identical IBA/water interfaces should be expected at the tube ends similar to the glycerol/water experiment, and the tubes are sufficiently long for the interfaces not to feel each other. Completing several test experiments, we found that the symmetry is broken at the time of immersion of the capillary tube into the water bath: the IBA/water interface always starts moving into the tube from the end that first touches the water. We should underline that the same initial conditions were realized in all our experiments with all binary mixtures. The fact that the removal of the IBA phase occurs differently is explained by different material constants of the IBA/water mixture (lower viscosity, diffusivity, and density contrast).

The spontaneous imbibition process should involve the hydrodynamic flow driven by the capillary pressure. To figure out the role of hydrodynamic flows we fulfilled the experiment with spherical glass particles with diameters in the range of $100 - 400\mu\text{m}$ dispersed into the IBA phase. The spheres are settled at the bottom wall of the tube. The evolution of the interface shape passing over the spheres is shown in figure 14. The interface shape is affected by the imposed obstacles but the interface regains its normal shape and continues its normal run in the tube's section without particles. From figure 14, one concludes that the particles are generally not engaged by

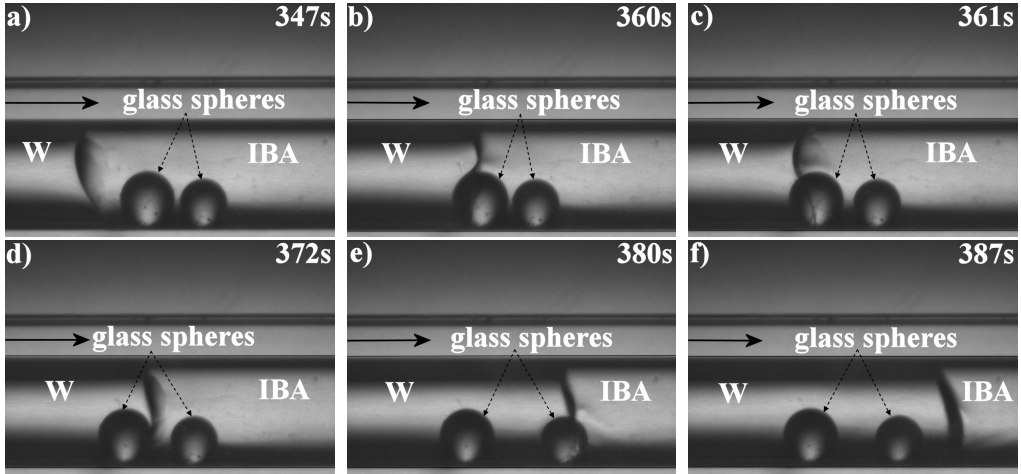


Figure 14: The shape of the IBA-water interface within a capillary tube of circular cross-section with the diameter of 0.6 mm and the length of 10 cm . The IBA phase contains spherical glass particles. The temperature is $T = 23^{\circ}\text{C}$.

the flow. Having watched the full video we may conclude that each particle is being moved only when the interface passes over the particle. The second particle is smaller, obviously has less inertia, and moved farther. Each particle moves first forwards, when the interface approaches the particle from the left, and then backwards, when the interface leaves the particle. Surprisingly, we detect no motion engaged by the fluid that should be pushed/pulled by the interface.

Finally, based on the sequence of snapshots we derived the speed of the interface propagation. Some values for the velocities of the interface within the smallest capillary tubes ($d = 0.2\text{ mm}$ and $d = 0.4\text{ mm}$) are shown in figure 15. In the initial moment the interface speed increases up to a limiting value that remains constant while the interface is moving through the middle section of the tube; the interface speed drops when the interface approaches the opposite end. The constant speed of the interface agrees with formula (6). The use of equation (6) allows us to estimate the capillary pressure in the tube of diameter $d = 0.2\text{ mm}$ being equal to 1 Pa . However, according to expressions (6) and (5), the speed of the interface should be proportional to the diameter of the tube, which was not observed. The speed of the interface grows with the increase of temperature.

Unfortunately, we could not obtain accurate measurements of the interface speeds at near-critical temperatures. The snapshots obtained for these

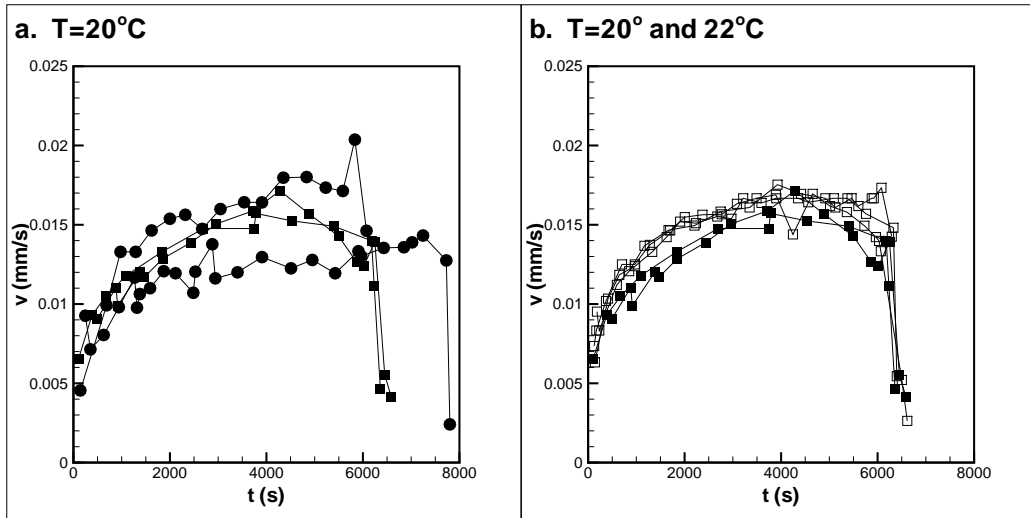


Figure 15: The speed of the IBA/water interface in under-critical conditions. a) Results for tubes of different diameters are shown, $d = 0.2\text{ mm}$ (■) and $d = 0.4\text{ mm}$ (●); the tubes have the length $L = 10\text{ cm}$, and the temperature is $T = 20^\circ\text{C}$. b) The results are for the same tube (diameter $d = 0.2\text{ mm}$ and length $L = 10\text{ cm}$) but under different temperatures, $T = 20^\circ\text{C}$ (■) and $T = 22^\circ\text{C}$ (□). Several different experiments are shown for every case.

conditions (e.g. figures 11b,e) indicate that the gravity effects become more important in driving the fluid flow. The diffusivity is low, and the interface motion is complex representing the interplay between the spontaneous imbibition and gravity current effects.

At supercritical temperatures the surface tension effects decrease, and the capillary force is not capable of displacing the IBA phase. The time evolution of the interfaces in supercritical conditions is shown in figure 16. Initially, the water phase moves into the tube from both ends under-riding the IBA phase. Being quite close to the tube ends one of the interfaces stops moving (figures 16d and 16f show the immovable interface). The other interface continues its motion (figure 16a-c,e), it diffuses faster and disappears much earlier than the second immovable interface (figure 16e shows one of the latest moments when the moving interface can still be distinguished; figure 16f depicts the clearly visible immovable interface at a much later time moment). The observed diffusion of the phase boundaries is not uniform along its length with the visible smearing starting at the tip.

In supercritical conditions IBA and water are miscible in any proportions. The way in which water penetrates into the capillary tube is different

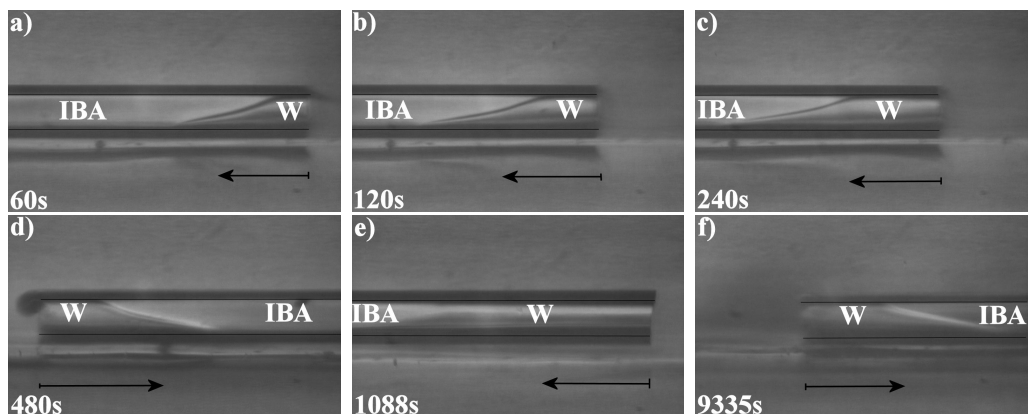


Figure 16: The interface shapes at different time moments within a capillary tube with diameter of 0.2 mm and length 10 cm . The temperature is $T = 27^{\circ}\text{C}$.

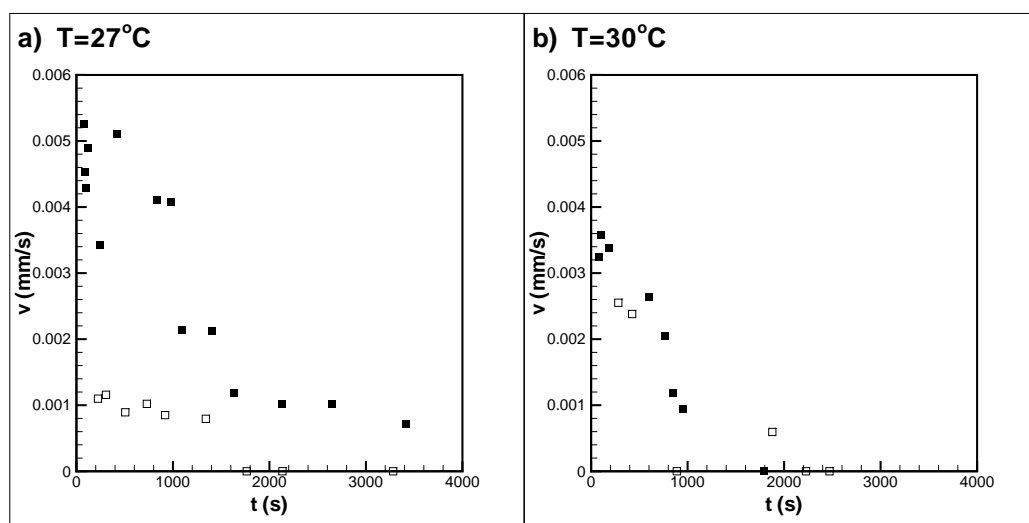


Figure 17: The speeds of the IBA/water interfaces in capillary tubes with the diameter of 0.2 mm and length 10 cm . The experiments were conducted at temperatures: a) $T = 27^{\circ}\text{C}$ and b) $T = 30^{\circ}\text{C}$. The filled symbols define the motion of one interface (which moves for longer time), while the empty symbols define the motion of the second interface from the opposite end of the tube.

from the observations outlined above for the other binary mixtures and for under-critical conditions. From one hand, the observed behaviour is non-symmetrical, similar to the undercritical observations, which might point out that the capillary or gravity forces can be important (the hydrodynamic motion initiated by the capillary/gravity forces is still significant due to the lower viscosity of the IBA/water mixture compared to the viscosities of glycerol/water and soybean oil/hexane mixtures). From the other hand, two interfaces at the opposite ends are observed, similar to the mixtures of glycerol/water and soybean oil/hexane. The observed motion of the IBA/water interfaces is quite irregular. The speeds of the two interfaces derived from the image sequences are shown in figure 17.

The measurements show that the speed of the first (moving) interface is comparable with the speed of glycerol/water interface in tubes of the same diameter. This suggests that the propagation of this interface is not driven by diffusion, since the diffusion coefficient of the IBA/water mixture is generally one order smaller than the diffusion coefficient for glycerol and water. The evolution of the second (immovable) interface is likely to be defined by diffusion but owing to low diffusivity it evolves very slowly.

4. Conclusions

We examined the shapes and dynamics of solute/solvent phase boundaries of three different binary mixtures in open horizontal capillary tubes. No pressure gradient was applied between the tube ends. Tubes of different diameters, as small as 0.2 mm were used. The task was to separate the interfacial diffusion from the hydrodynamic flows driven by either Marangoni or solutal convection, or by the capillary pressure (the spontaneous imbibition). Traditionally, the dissolution process is reduced to a simple interphase diffusion. A classically expected scenario for the dissolution of a solute droplet from a capillary tube would be as follows: two solute/solvent interfaces are formed at the tube ends, if no external pressure gradient is applied, no flows should be generated and hence the phase boundaries should not move, and the boundaries will smear and finally disappear due to diffusion. We found that removal of solute phase occurs differently. Firstly, numerous physical phenomena are involved at different stages of our seemingly simple experiments. Secondly, even diffusion dynamics of the solute/solvent interfaces differs from general expectations.

We managed to isolate the pure dissolution process in the experiments with mixtures of glycerol/water and soybean oil/hexane mixtures. The short initial evolution (for about 1 *min*, when diffusion is negligible) is gravity driven; the observed motion represents a gravity current also called a lock-exchange flow [28, 29, 30]. The contact lines are not closed within the tube, the solvent phase displaces small portions of the solute at both ends. But when the interfaces enter the tube and the contact lines become closed within the tube, the solute phase becomes locked. At this moment the gravity force is balanced by the capillary force, which ends the initial ‘mechanical’ displacement of the solute phase. From this moment, whole interfaces with almost steady shapes move into the tube’s centre, which obviously cannot be interpreted as a gravity current. These phase boundaries smear in time seemingly due to mutual interphase diffusion, but the smearing rate is very small, considerably smaller compared to the speed of the boundary movement as a whole. The observed motion of the phase boundaries resembles the evaporation or solidification process: the interfacial mass transfer results in shrinking of the solute droplet, but the solute/solvent boundaries remain visible (if not sharp). The two interfaces move with equal speeds. The speeds of the interfaces slow down following the $t^{-2/3}$ power law in the tubes of smaller diameters, i.e. do not follow the predictions of the diffusion theory, $t^{-1/2}$. The dissolution rate increases with growth of temperature, which was expectable, but we also found that the rate of decrease of the droplet’s length is proportional to the area of the tube’s cross-section, which is a surprising result. Finally, we conclude that the phase boundaries are moving due to barodiffusion.

The observed meniscus shapes allow us to propose an estimate of the surface tension coefficient for the soybean oil/hexane mixture, which should be of the order of $0.1 \text{ dyn} \times \text{cm}^{-1}$. Comparing the interface speeds, we may also conclude that the diffusion coefficient of the soybean oil/hexane mixture is obviously higher than the diffusion coefficient of the glycerol/water interface, which agrees with theoretical predictions [53]. Moreover, the values of the diffusion coefficients reported in the literature allowed us to conclude that the speed of the interface is proportional to $D^{1/3}$.

The behaviour of the IBA/water mixture was different. Below the critical point the mixture can be heterogeneous in equilibrium. But the amount of IBA enclosed in the capillary tube was negligible in comparison with the volume of the water bath, and consequently is fully dissolvable. Nevertheless, we found that IBA and water behaved like two immiscible liquids in the

experiments carried out below the critical temperature. Water penetrated into the tube from one side; from another side IBA droplets were displaced. The droplets were detached when their size was sufficient to overcome the adhesion to the tube's outer wall. The speed of the interface propagation grew in the beginning up to a constant value, then the speed remained constant for the main part of the experiment and sharply decreased when the interface approached the second end of the tube. The motion of the interface was explained by spontaneous imbibition. In the experiments with the micro-particles dispersed in the IBA phase, we observed that the interface was able to move the particles, but the fluid that should be driven by the interface did not force the particles to move.

Above the critical point, IBA and water are miscible in all proportions. The observed meniscus shape was defined by the balance of the capillary and gravity forces, which seemed comparable. The capillary pressure was not sufficiently strong to initiate the spontaneous imbibition. The initial evolution of the interfaces could be explained by the gravity action. Two interfaces were observed within the tube. One of them was initially moving but quickly became very diffusive and indistinguishable. The other interface was observed for considerably longer time periods but it remained stationary.

The diffusion and viscosity coefficients and density contrast between mixture components for the IBA/water binary mixture are considerably lower in comparison to those of glycerol/water and soybean oil/hexane mixtures, both below and above the critical point. Below the critical point, the interfacial diffusion at the IBA/water boundaries was not observed at all. The interface speed is comparable to the initial speeds of glycerol/water and soybean oil/hexane interfaces, but the solute is removed faster as the speed of the undercritical IBA/water interface remains almost constant for the duration of the experiment. Above the critical point, two IBA/water interfaces penetrate into the tube, and their motion should be driven by mechanisms similar to those that govern the motion of glycerol/water and soybean oil/hexane interfaces. But, seemingly, owing to smaller diffusion and viscosity coefficients, and smaller density contrast the supercritical IBA/water phase boundaries move differently.

Finally, we would like to note that the interface shapes and dissolution dynamics were qualitatively the same in tubes of different cross-section, in tubes made of different materials, and in new tubes and tubes previously used for the experiments and then washed with water and acetone and dried out. Bulk interfaces and contact lines always moved with the same speeds.

No visible solute remained left on the walls of the tube after the interface passage. Owing to gravity effect, in the horizontal capillary tubes, the apparent contact angles are different at the lower and upper parts of the tube. In the case of IBA/water mixtures, the contact angles obviously depend on the mixture temperature.

The collected experimental data should be useful for developing the theoretical models for multiphase flows with undergoing phase transformations. For instance, in most current models (e.g. [26]), the dissolution of completely miscible binary mixtures is modelled with the use of the Fickian law, and the barodiffusion and capillary effects are disregarded.

5. Acknowledgments

This work is done within the framework of the EPSRC project EP/G014337 ‘Pore-level Network Modelling of the Miscible Displacement’. The authors thank Dr. J. Shrimpton and Dr. Dehao Ju for helping with the optical measurements.

References

- [1] M. Mukhopadhyay, Natural extracts using supercritical carbon dioxide, CRC Press LLC, 2000.
- [2] E. C. Donaldson, G. V. Chilingarian, T. F. Yen, Enhanced Oil Recovery, Elsevier, New York, 1985.
- [3] T. Babadagli, Journal of Petroleum Science and Engineering 57 (2007) 221–246.
- [4] J. W. Jawitz, M. D. Annable, P. S. C. Rao, Journal of Contaminant Hydrology 31 (1998) 211–230.
- [5] A. Silva, C. Delerue-Matos, A. Fiuza, Journal of Hazardous Materials 124 (2005) 224–229.
- [6] M. Sahimi, Reviews of Modern Physics 65 (1993) 1393–1534.
- [7] S. H. Vanaparthi, E. Meiburg, European Journal of Mechanics B-Fluids 27 (2008) 268–289.

- [8] A. Dokoumetzidis, P. Macheras, *International Journal of Pharmaceutics* 321 (2006) 1–11.
- [9] E. Aker, K. J. Maloy, A. Hansen, G. G. Batrouni, *Transport in Porous Media* 32 (1998) 163–186.
- [10] M. J. Blunt, M. D. Jackson, M. Piri, P. H. Valvatne, *Advances in Water Resources* 25 (2002) 1069–1089.
- [11] D. J. Korteweg, *Archives Neerlandaises des Sciences Exactes et Naturelles* 6 (1901) 1–24.
- [12] Y. B. Zeldovich, *Zhur. Fiz. Khim.* XXIII (1949) 931–935.
- [13] D. D. Joseph, Y. Y. Renardy, *Fundamentals of two-fluid dynamics. Part II: Lubricated transport, drops and miscible liquids*, Springer-Verlag, Berlin, 1993.
- [14] S. E. May, J. V. Maher, *Physical Review Letters* 67 (1991) 2013–2016.
- [15] J. A. Pojman, C. Whitmore, M. L. T. Liveri, R. Lombardo, J. Marszalek, R. Parker, B. Zoltowski, *Langmuir* 22 (2006) 2569–2577.
- [16] B. Zoltowski, Y. Chekanov, J. Masere, J. A. Pojman, V. Volpert, *Langmuir* 23 (2007) 5522–5531.
- [17] L. Lacaze, P. Guenoum, D. Beysens, M. Delsanti, P. Petitjeans, P. Kurowski, *Physical Review E* 82 (2010) 041606.
- [18] J. A. Pojman, N. Bessonov, V. Volpert, *Microgravity Science and Technology XIX* (2007) 33–41.
- [19] L. D. Landau, E. M. Lifshitz, *Course of theoretical physics. Vol. 6. Fluid Mechanics*, Elsevier. Butterworth Heinemann, 2009.
- [20] M. Giglio, A. Vendramini, *Physical Review Letters* 35 (1975) 168–170.
- [21] F. B. Hicks, T. C. V. Vechten, C. Franck, *Physical Review E* 55 (1997) 4158–4164.
- [22] A. Vailati, M. Giglio, *Physical Review E* 58 (1998) 4361–4371.

- [23] J. Lowengrub, L. Truskinovsky, *Proceeding of the Royal Society of London A* 454 (1998) 2617–2654.
- [24] G. Viner, J. A. Pojman, *Optics and Lasers in Engineering* 46 (2008) 893–899.
- [25] A. Vorobev, *Physical Review E* 82 (2010) 056312.
- [26] C.-Y. Chen, E. Meiburg, *Journal of Fluid Mechanics* 326 (1996) 57–90.
- [27] V. V. Ugrozov, A. N. Filippov, C. A. Paraskeva, G. N. Constantinides, V. M. Starov, *Colloids and Surfaces A: Physicochemical and Engineering Aspects* 239 (2004) 129–133.
- [28] E. E. Zukoski, *Journal of Fluid Mechanics* 25 (1966) 821–837.
- [29] T. B. Benjamin, *Journal of Fluid Mechanics* 31 (1968) 209–248.
- [30] R. J. Lowe, J. W. Rottman, P. F. Linden, *Journal of Fluid Mechanics* 537 (2005) 101–124.
- [31] E. W. Washburn, *Physical Review* 17 (1921) 273–283.
- [32] R. Chertcoff, A. Calvo, I. Paterson, M. Rosen, J. Hulin, *Journal of Interface and Colloid Science* 154 (1992) 194–201.
- [33] G. I. Taylor, *Journal of Fluid Mechanics* 10 (1961) 161–165.
- [34] B. G. Cox, *Journal of Fluid Mechanics* 14 (1962) 81–96.
- [35] B. G. Cox, *Journal of Fluid Mechanics* 20 (1964) 193–200.
- [36] E. J. Soares, M. S. Carvalho, P. R. S. Mendes, *Journal of Fluids Engineering* 127 (2005) 24–31.
- [37] P. Petitjeans, T. Maxworthy, *Journal of Fluid Mechanics* 326 (1996) 37–56.
- [38] J. Kuang, T. Maxworthy, P. Petitjeans, *European Journal of Mechanics-B/Fluids* 22 (2003) 271–277.
- [39] J. Kuang, T. Maxworthy, P. Petitjeans, *Experiments in Fluids* 37 (2004) 301–308.

- [40] J. Dambrine, B. Geraud, J.-B. Salmon, *New Journal of Physics* 11 (2009) 075015.
- [41] B. Chu, F. J. Schoenes, W. P. Kao, *Journal of the American Chemical Society* 90 (1968) 3042.
- [42] T. S. Venkataraman, L. M. Narducci, *Journal of Physics C: Solid State Physics* 10 (1977) 2849–2861.
- [43] J. B. Segur, H. E. Oberstar, *Industrial and Engineering Chemistry* 43 (1951) 2117–2120.
- [44] N. Ouerfelli, T. Kouissi, N. Zrelli, M. Bouanz, *Journal of Solution Chemistry* 38 (2009) 983–1004.
- [45] J. Kim, Y. S. Ju, in: *Micro Electro Mechanical Systems 2008, MEMS2008, Proceedings of IEEE 21st International conference*, Tucson AZ, USA, pp. 587–590.
- [46] N. Rashidnia, R. Balasubramaniam, *Experiments in Fluids* 36 (2004) 619–626.
- [47] G. D’Errico, O. Ortona, F. Capuano, V. Vitagliano, *Journal of Chemical Engineering Data* 49 (2004) 1665–1670.
- [48] B. Chu, F. Schoenes, *Physical Review Letters* 21 (1968) 6.
- [49] R. L. Rowley, F. H. Horne, *The Journal of Chemical Physics* 71 (1979) 3841.
- [50] N.-C. Wong, C. M. Knobler, *Physical Review A* 24 (1981) 3205–3211.
- [51] U. Kaatze, S. Z. Mirzaev, *The Journal of Physical Chemistry A* 104 (2000) 5430–5436.
- [52] R. G. Howland, N.-C. Wong, C. M. Knobler, *Journal of Chemical Physics* 73 (1980) 522–531.
- [53] J. C.-S. Wu, E.-H. Lee, *Journal of Membrane Science* 154 (1999) 251–259.
- [54] J. Crank, *The mathematics of diffusion*, Clarendon Press, Oxford, 1976.
- [55] D. S. Cohen, A. B. White, *SIAM J. Appl. Math.* 51 (1991) 472–483.